



U.S. DEPARTMENT OF
ENERGY

Office of
Science

DOE/SC-ARM-14-018

Field Evaluation of Real-time Cloud OD Sensor TWST during the DOE ARM TCAP Campaign 2013 Final Campaign Report

E Niple
J Conant
S Jones

H Scott
F Iannarilli

February 2016



DISCLAIMER

This report was prepared as an account of work sponsored by the U.S. Government. Neither the United States nor any agency thereof, nor any of their employees, makes any warranty, express or implied, or assumes any legal liability or responsibility for the accuracy, completeness, or usefulness of any information, apparatus, product, or process disclosed, or represents that its use would not infringe privately owned rights. Reference herein to any specific commercial product, process, or service by trade name, trademark, manufacturer, or otherwise, does not necessarily constitute or imply its endorsement, recommendation, or favoring by the U.S. Government or any agency thereof. The views and opinions of authors expressed herein do not necessarily state or reflect those of the U.S. Government or any agency thereof.

**Field Evaluation of Real-time Cloud
OD Sensor TWST during the
DOE-ARM-TCAP Campaign 2013
Final Campaign Report**

E Niple, Aerodyne Research
H Scott, Aerodyne Research
J Conant, Aerodyne Research
F Iannarilli, Aerodyne Research
S Jones, Aerodyne Research

February 2016

Work supported by the U.S. Department of Energy,
Office of Science, Office of Biological and Environmental Research

Summary

The objective of this internal research and development (IRAD)-funded campaign by Aerodyne Research, Inc. was to demonstrate the field-worthiness and assess the performance of a real-time cloud optical depth (COD) sensor (dubbed three-waveband spectrally-agile technique [TWST]) through a side-by-side comparison with proven, ground-based operational sensors currently deployed at the U.S. Department of Energy (DOE) Atmospheric Radiation Measurement (ARM) Climate Research Facility Mobile Facility (AMF) site on the Cape Cod National Seashore for the Two-Column Aerosol Project ([TCAP](#)). We anticipated direct comparisons with the Aerosol Robotic Network (AERONET; when in cloud mode) and SAS instruments and expected ancillary data from other sensors such as the Total Sky Imager, the Scanning Cloud Radar, and the Microwave Radiometer to facilitate and validate these comparisons. Because the cloud optical depth retrieval algorithms used by AERONET, solar array spectrometer (SAS), and TWST are totally independent, this deployment provided a unique opportunity to evaluate the field performance of TWST. If the effort proves successful, it may qualify TWST for operational service or additional evaluation effort.

Although TWST is based on the same principle of operation as the Cloud Mode¹ AERONET sensor,² it offers certain key advantages in the measurement of COD. These advantages stem from two fundamental differences. First, TWST is dedicated to COD measurement, while the AERONET CIMEL sunphotometer was designed primarily for aerosol optical depth and later adapted for COD measurements. Second, the TWST design is based on a compact spectrometer using a linear focal plane array detector, whereas the CIMEL sunphotometer is currently limited to six (or eight, for latest version) spectral filter bands. These differences result in three strengths in favor of TWST for COD measurements: high temporal resolution, high spatial resolution, and high spectral resolution.

High temporal resolution, 1 second (sec) or less vs. 90 sec. Although the AERONET Cloud Mode collects a full sample in 9 sec, the cloud mode averaging technique (herein referred to as a “trimmed mean”) requires 10 full samples to generate one data point. The TWST spectrometer that senses all spectral resolution elements simultaneously provides a valuable multiplex advantage. As a result, TWST can collect samples at least one to two orders of magnitude faster without sacrificing signal-to-noise ratio (SNR) and thereby capture more effectively the fast evolution of cloud properties. To make the TWST temporal advantage-specific, we indicate that for each TWST data point (at a 1 hertz [Hz] sample rate), the radiance values collected at 440 and 870 nanometers (nm) are truly simultaneous, whereas there is a 4-sec delay between the radiance values collected for the same two bands in the AERONET CM. This lack of simultaneity can introduce substantial unwanted errors into the COD measurements for rapidly evolving clouds. More detail on this point is provided in section 4.3.2.

High spatial resolution, 0.5 degrees (deg) vs. 1.2 deg. This reduces clear sky background contamination and promotes the study of cloud edges where cloud-aerosol interactions are an important effect.

¹ Chiu, JC, C-H Huang, A Marshak, I Slutsker, DM Giles, BN Holben, Y Knyazikhin, and WJ Wiscombe. 2010. “Cloud optical depth retrievals from the Aerosol Robotic Network (AERONET) cloud mode observations.” *Journal of Geophysical Research: Atmospheres* 115(D14202), doi:10.1029 /2009JD013121.

² Holben, BN, TF Eck, I Slutsker, D Tanré, JP Buis, A Setzer, E Vermote, JA Reagan, YJ Kaufman, T Nakajima, F Lavenu, I Janowiak, and A Smirnov. 1998. “AERONET—A federated instrument network and data archive for aerosol characterization.” *Remote Sensing of the Environment* 66: 1–16.

High spectral resolution, approximately 300 spectral resolution elements vs. 6 spectral bands. Again, the spectrometer puts more spectral information into the hands of the analyst leading to higher sensitivity, enabling the extraction of more precise cloud optical depths.

TWST data were collected on 37 days from 17 May to 27 June 2013. The preliminary (Level 1) TWST results are compared to AERONET spectral radiances (Figure 1) and COD measurements from the AERONET Cloud Mode sensor (Figure 2) and to the microwave radiometer (MWR) sensor.

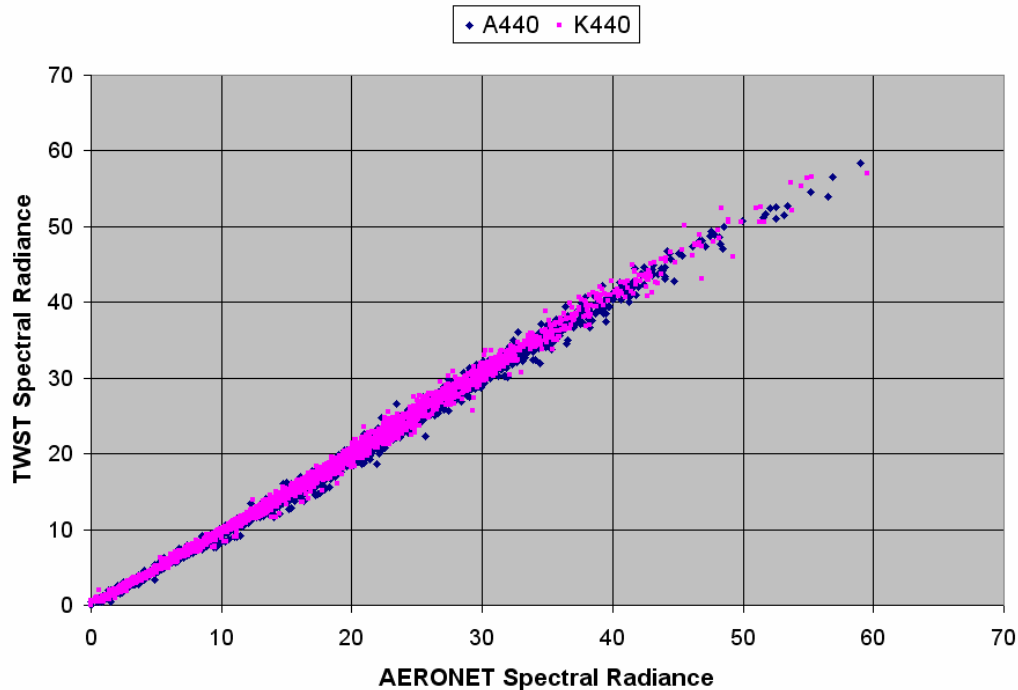


Figure 1. Summary comparison of AERONET and TWST Spectral Radiances ($\mu\text{W}/\text{centimeters [cm]}^2 \text{sr nm}$) at 440 nm over a 37-day field measurement period.

Figure 1 indicates good coincidence of TWST 440 nm spectral radiance calibration with AERONET. Likewise, over a wide variety of cloud optical depths, Figure 2 indicates that TWST and AERONET generally agree on the extracted optical depths, albeit using independent algorithms. We attribute the relatively moderate disparities between TWST and Cloud Mode AERONET optical depths to two sources: slightly different field of view (FOV) footprints overhead, and differing measurement periods, both of which exacerbate differences in the presence of fast-moving broken clouds. Spurious differences can arise from clock skew between sensors even though we have taken care to minimize this effect. The close agreement between the two sensor calibrations as indicated in Figure 1 eliminates calibration as a potential factor.

Figure 2 reveals a few occurrences with large disparities in optical depth readings; their causes are examined in some detail within this report. Many of these cases falling near zero on one of the plot axes clearly signals that they are likely the result of the “thick vs. thin cloud” ambiguity.

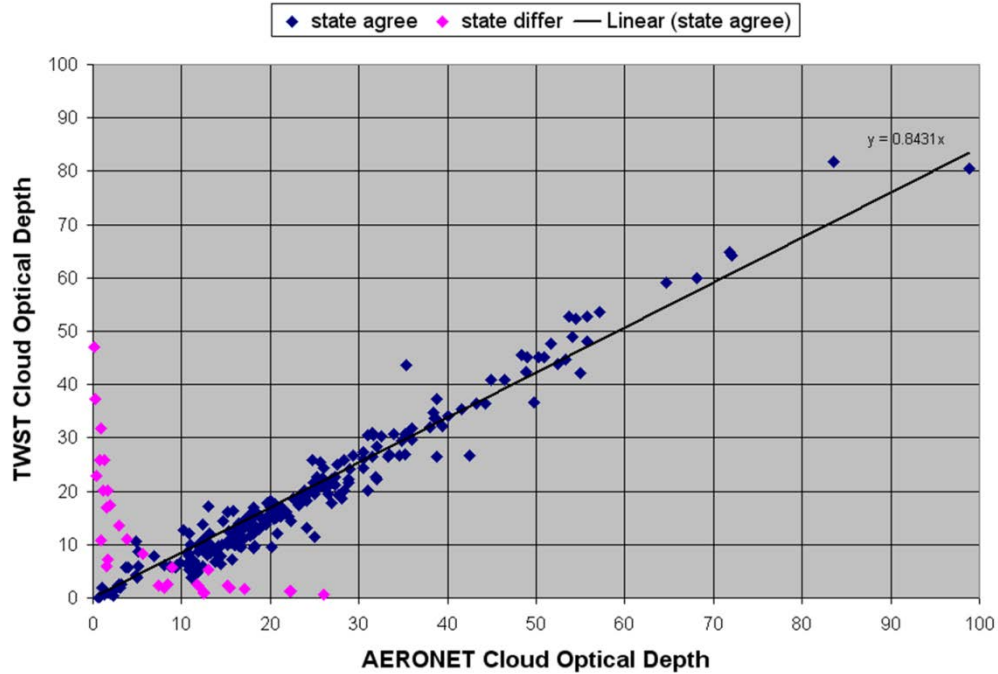


Figure 2. Comparison of AERONET Cloud Mode to TWST CODs for a 37-day field measurement period. Cloud state refers to the “thick or thin” choice made by the AERONET and TWST COD retrieval algorithms.

To make the appropriate comparison of like quantities in Figure 2, we found it important to understand the “trimmed mean” technique used by the AERONET cloud mode to extract a single value from the 10 points collected in each 90-second sample period. This scenario required us to apply the AERONET Cloud Mode averaging technique to each 90 sec (90 points) of TWST data to create the comparison. Using the same cloud mode averaging technique with the TWST data allowed us to arrive at a quantitative measure of agreement between the AERONET CM and the TWST cloud optical depth results. After excluding the data points at low optical depth (OD; in pink), where the AERONET and TWST algorithms are more apt to disagree on the cloud state, the remaining 235 data points (blue diamonds) yield a respectable rms-deviation of OD 3.2.

Acknowledgments

We want to thank the MAGIC PI Dr. Ernie Lewis/Brookhaven National Laboratory (BNL) and Dr. Christine Chiu of University of Reading, UK for strongly suggesting and pointing us toward the TCAP field test opportunity, the TCAP PI Dr. Larry Berg/PNNL, and Paul Ortega/Los Alamos National Laboratory (LANL) for guiding us through the deployment procedures. We would especially like to thank Mr. Vaughan Ivens for on-site support in setting up and making periodic status checks on TWST. We appreciate the assistance of Dr. Maria Cadeddu of Argonne National Laboratory in interpreting the microwave radiometer (MWR) data. We thank Dr. Connor Flynn of PNNL for his suggestions and encouragement. Data were obtained from the ARM Climate Research Facility sponsored by the U.S. Department of Energy (DOE), Office of Science, Office of Biological and Environmental Research, Climate and Environment Sciences Division. We thank Laurie Gregory and Richard Wagener of BNL for suggestions in interpreting the CIMEL Sunphotometer data that were collected by DOE as part of the ARM Climate Research Facility and processed by the National Aeronautics and Space Administration's (NASA's) Aerosol Robotic Network (AERONET). Finally, we want to acknowledge the initial support and motivation for the development of the TWST Cloud Optical Depth Sensor from the Air Force Research Laboratory/Dr. Wellesley Pereira.

Acronyms and Abbreviations

AERONET	NASA's Aerosol Robotic Network
AMF	ARM Mobile Facility
ARM	Atmospheric Radiation Measurement
BNL	Brookhaven National Laboratory
cm	centimeter(s)
COD	cloud optical depth
deg	degree(s)
DOE	U.S. Department of Energy
FOV	field of view
Hz	hertz
IRAD	internal research and development
LANL	Los Alamos National Laboratory
MWR	microwave radiometer (sensor)
NASA	National Aeronautics and Space Administration
nm	nanometer(s)
OD	optical depth
SAS	solar array spectrometer
sec	second(s)
SNR	signal-to-noise ratio
TCAP	Two-Column Aerosol Project
TSI	Total Sky Imager (camera)
TWST	three-waveband spectrally-agile technique

Contents

Summary	iii
Acknowledgments.....	vi
Acronyms and Abbreviations	vii
1.0 Introduction	1
1.1 Three Waveband Spectrally-agile Technique Overview.....	1
1.1.1 Principle of Operation	1
1.1.2 TWST Hardware	3
1.1.3 TWST Software.....	4
1.1.4 Calibration.....	4
1.1.5 Conversion of Spectral Radiance to COD.....	5
2.0 Data Collection.....	5
2.1 Experimental Setup	5
2.2 Data Matrix	6
3.0 Results	7
3.1 Calibration Stability	7
3.2 Daily TWST Cloud Optical Depth Results.....	7
3.3 Comparison to Other Sensors.....	8
3.3.1 MWR, AERONET, and TWST.....	8
3.3.2 AERONET and TWST.....	11
4.0 Conclusions	17
Appendix A : TWST Digital Data Description.....	A.1
Appendix B : TWST Cloud OD Sensor Specifications	B.1

Figures

1. Summary comparison of AERONET and TWST Spectral Radiances at 440 nm over a 37 day field measurement period.....	iv
2. Comparison of AERONET Cloud Mode to TWST Cloud Optical Depths for a 37 day field measurement period.....	v
3. Schematic representation of zenith spectral radiance versus cloud optical depth.....	1
4. Schematic representation of photon pathlength versus cloud optical depth.....	2
5. Combination of the two previous figures to show the relationship between spectral radiance at 440 nm and the oxygen A-band equivalent width as the Cloud Optical Depth increases.	3
6. The TWST sensor hardware.	4
7. Location of TWST, AERONET, TSI and SAS at ARM Highlands site Cape Cod, MA. All sensors were heavily anchored in place to survive the high wind conditions.....	5
8. TWST Data Matrix for May 2013 at ARM Highlands site, Cape Cod, MA.....	6
9. TWST Data Matrix for June 2013 at ARM Highlands site, Cape Cod, MA.....	6
10. TWST Calibration Stability relative to calibration run on 17 May 2013.	7
11. Comparison of Cloud Optical Depths between TWST and MWR on 18 May 2013 in the morning.....	9
12. Comparison of Cloud Optical Depths between TWST, MWR and AERONET on 18 May 2013 in the afternoon.....	9
13. Comparison of Cloud Optical Depths between TWST and MWR on 19 May 2013 in the morning.....	10
14. Comparison of Cloud Optical Depths between TWST, MWR and AERONET on 19 May 2013 in the afternoon.	10
15. Comparison of Cloud Optical Depths between TWST, MWR and AERONET on 20 May 2013 in the early morning.	11
16. Comparison of Cloud Optical Depths and related parameters between TWST and AERONET on 12 June 2013 in the afternoon.	12
17. TSI images of the sky at ARM Highlands on 12 June 2013 at two times during the collection of AERONET data at 21:38 GMT.....	12
18. Comparison of Cloud Optical Depths between TWST and AERONET on 14 June 2013 in the afternoon.	13
19. TSI images of the sky at ARM Highlands on 14 June 2013 at the times of collection of AERONET data at 19:14 GMT.	14
20. Nose Plot of TWST measurements for the thirty minutes containing the time of the AERONET data collection on 14 June 2013 at 19:14 GMT.....	14
21. Spectral Radiance at 440 nm for AERONET Cloud Mode and TWST.....	15
22. TWST and AERONET Cloud Mode Cloud Optical Depths corresponding to the spectral radiances in the previous figure.	15
23. Comparison of AERONET Cloud Mode to TWST Cloud Optical Depths for a 37 day field measurement period.....	16

1.0 Introduction

1.1 Three Waveband Spectrally-agile Technique Overview

1.1.1 Principle of Operation

TWST expands on the AERONET approach so as to be used for a greater variety of terrains, to be easily portable, and to provide a COD measurement every second. A visible-band spectro-radiometer stares at a narrow segment (0.5 deg) of the sky directly overhead, recording the spectral radiance from 340 to 1023 nm wavelength with about 2 nm spectral resolution. The spectral radiance at 440 nm is the primary quantity needed for determining the cloud optical depth. The relationship between spectral radiance and cloud optical depth is two-valued (Figure 3); i.e., for each spectral radiance value, there are two cloud optical depths that correspond to that value. One is in the optically thin region, where the brightness increases with increasing cloud optical depth; the other is in the optically thick region, where the brightness decreases with increasing cloud optical depth. This COD ambiguity is the principal complication of using spectral radiances.

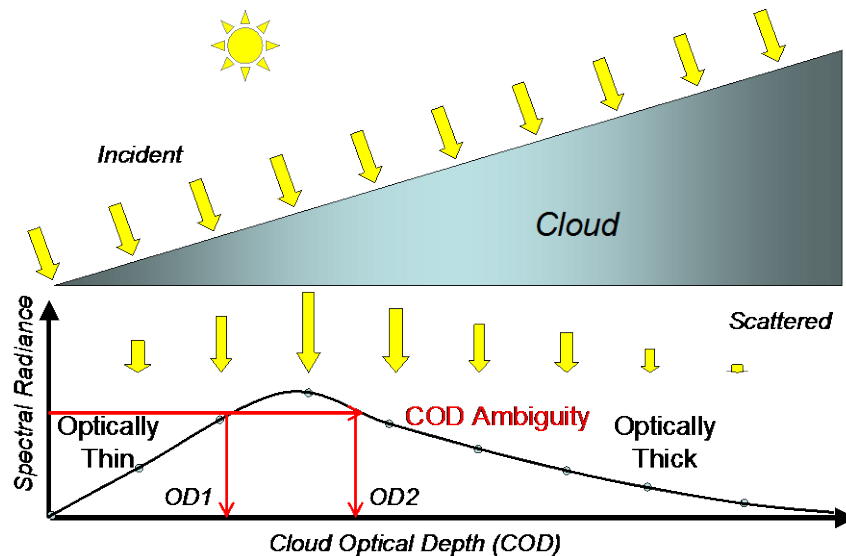


Figure 3. Schematic representation of zenith spectral radiance vs. cloud optical depth (COD). Clouds with CODs of OD1 and OD2 have the same up-looking radiance. This is the COD ambiguity and makes it impossible to relate a single COD for a given spectral radiance.

AERONET uses dual CIMEL sun photometers with spectral filter wheels and robotic pointing (see the [AERONET website](#) for details). Cloud Mode uses the 440 nm and 870 nm filters, as two bands were chosen to maximize the so-called “red-edge” albedo of vegetation to produce different brightness versus cloud optical depth curves and thereby resolve the COD ambiguity. Newer CIMEL photometers that

include a filter at 1640 nm are now being fielded, allowing the retrieval of cloud droplet size and liquid water path without requiring a vegetated surface albedo.¹

TWST uses a spectro-radiometer in place of the filter band radiometer to record 2048 spectral channels simultaneously. This gives TWST the spectral agility to use any band as the primary band for determining the cloud optical depth. In addition, it allows TWST to measure the equivalent width of the 760 nm oxygen A-band and thereby to resolve the COD ambiguity. The equivalent width is a monotonic function of the photon total path length and of the cloud optical depth; thus, it does not suffer from the COD ambiguity (Figure 5).²

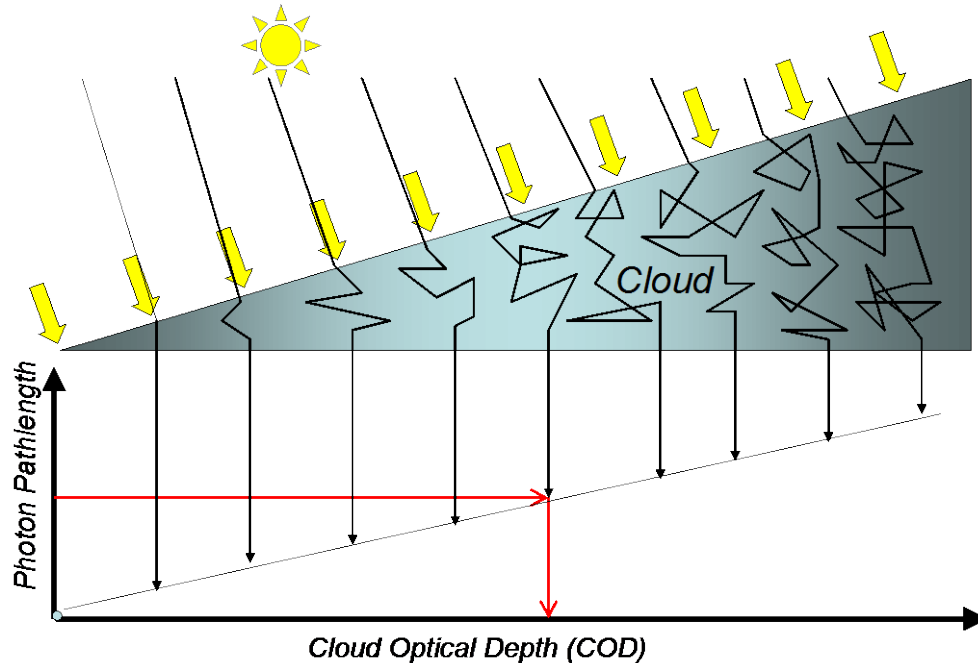


Figure 4. Schematic representation of photon pathlength vs. (COD), which is unambiguously mapped to the photon pathlength and hence the oxygen A-band equivalent width.

One way to use the equivalent width to resolve the COD ambiguity is by the nose plot. Because spectral radiance at 440 nm is two-valued and equivalent width of oxygen A-band is monotonic in COD, plotting equivalent width versus spectral radiance at 440 nm for a series of times during evolution of the COD traces out a characteristic nose-like curve (Figure 5). The point of maximum spectral radiance, the tip of the nose, divides the CODs into optically thin and thick regions easily differentiated by the direction of change in the equivalent width values. The slope of the curve is positive when the cloud is optically thin and negative when the cloud is optically thick. Also characteristic is the higher absolute slope in the optically thick case. As a cloud evolves its location, the nose plot traces out a portion of the curve. The state of the cloud (i.e., whether it is optically thin or optically thick) can thus be determined by the sign of the slope of the curve traced out, providing the time step is short relative to the cloud's evolution.

¹ Chiu, JC, A Marshak, C-H Huang, T Várnai, RJ Hogan, DM Giles, BN Holben, EJ O'Connor, Y Knyazikhin, and WJ Wiscombe. 2012. "Cloud Droplet Size and Liquid Water Path Retrievals from Zenith Radiance Measurements: Examples from the Atmospheric Radiation Measurement Program and the Aerosol Robotic Network." *Atmospheric Chemistry and Physics Discussions* 12:8, 19163–19208, [doi:10.5194/acpd-12-19163-2012](https://doi.org/10.5194/acpd-12-19163-2012).

² The Cosmos astronomy encyclopedia can be referenced for additional information about [equivalent width](#).

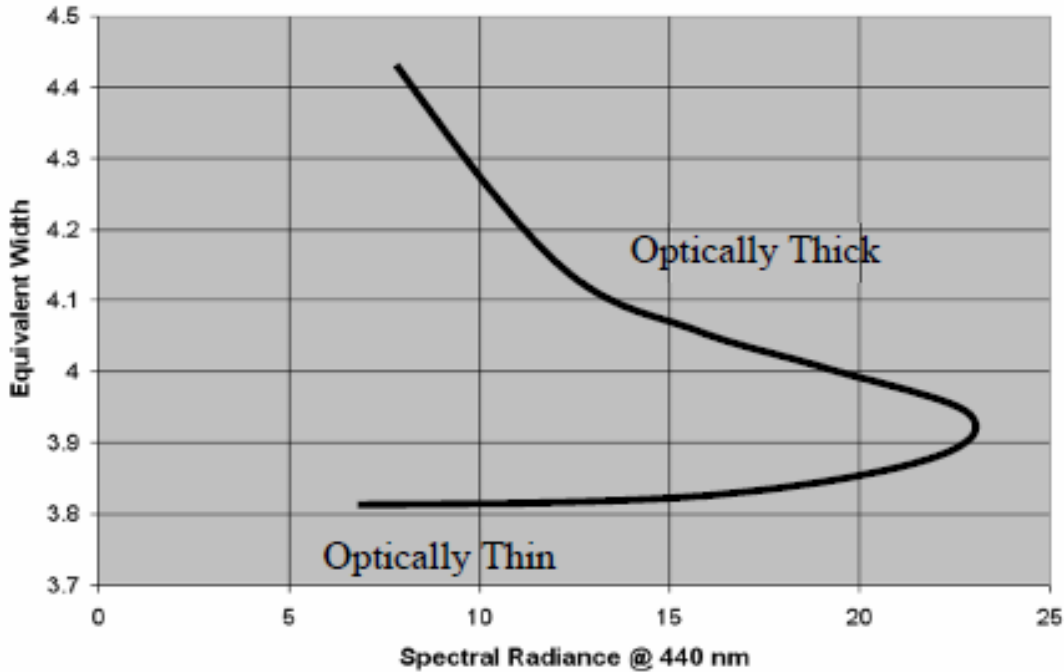


Figure 5. Combination of the two previous figures to show the relationship between spectral radiance (in $\mu\text{W}/\text{cm}^2 \text{sr nm}$) at 440 nm and the oxygen A-band equivalent width (in nm) as the COD increases.

Of course, other factors cause equivalent width to change besides COD. Changes in the solar zenith angle produce decreases in equivalent width with time during the morning and increases in the afternoon. Changes in the density-weighted average cloud thickness and cloud altitude also affect the equivalent width independent of the COD. When the COD is changing slowly but the solar zenith angle and cloud thickness are changing more quickly, the nose plot can become complex and difficult to interpret. Also, it can be distorted by various 3D cloud effects.

1.1.2 TWST Hardware

The TWST sensor consists of three main components (Figure 6). The first is the sun baffle (20 cm in length) that prevents scattered off-axis radiation from reaching the detector. A slanted optical window at the upper end of the baffle tube sheds rain and other forms of precipitation. The second is the optical head, consisting of a compact spectro-radiometer connected by an optical fiber to a collecting lens focused at infinity. A computer controlled shutter provides for frequent dark current correction. A solid tripod mount holds the sensor, which is carefully aligned and pointed to zenith. The third component is the controlling computer that collects the output from the sensor, stores it, and computes the COD.

- 20 lbs
- 5 hr battery life
- Weather proof (NEMA 4)
- Automated operation
- 1 Hz sample rate
- 0.5 deg FOV

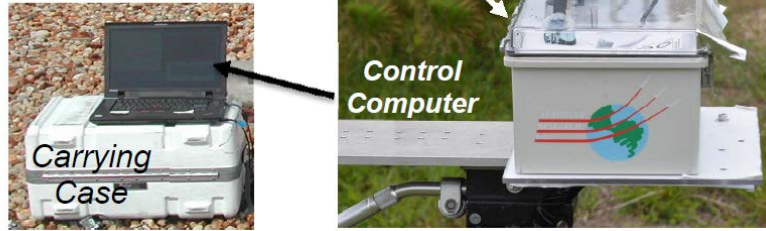


Figure 6. The TWST sensor hardware.

1.1.3 TWST Software

The software that logs the data and produces the real-time output is one of several modules needed by TWST. A set of utilities is combined into an analysis package that produces calibration files, plots individual spectra, surveys sequences of spectra, and provides advanced post-processing. A batch processing module that processes many weeks of data at a time without operator intervention is new for the TCAP test.

1.1.4 Calibration

There are two forms of calibration that must be managed for any technique that uses spectro-radiometers: wavelength and radiometric. The wavelength calibration of compact grating spectrometers like the one used in TWST has proven stable over periods of months. This assumes that the spectrometer has suffered no major physical shocks. On the other hand, radiometric calibration stability is usually not well characterized by the manufacturer and must be confirmed by long-term testing. We started out performing a calibration in the morning, taking data around mid-day, and then calibrating again in the evening. When this method was shown to be stable, we moved to increasingly longer test periods. Over a series of tests, we were able to extend our procedure to include shipping (with careful packing) to and from a remote test site and several hours of testing over 3 days. This was pushed to a new level by the test procedure required for TCAP. For this deployment, the sensor was exposed to the elements for several weeks (17 May to 27 June).

Our calibration procedure utilizes a LabSphere URS-600 Uniform Radiance Standard Source. The source and the TWST sensor are allowed about 20 min to stabilize. A series of from 10 to 20 different data points are then collected while monitoring the total flux recorded by the source internal flux sensor, which is used to adjust for first-order lamp aging. Some spectral drift remains uncorrected. Multiple

measurements at the target TWST integration time of 5,000 μsec , as well as measurements at larger and smaller integration times, are made. The manufacturer's calibration data is then used to produce a calibration coefficient at each wavelength. The results are stored in a calibration file that ships with the sensor.

1.1.5 Conversion of Spectral Radiance to COD

TWST uses a database of computed spectral radiances versus solar zenith angle at various CODs to perform the conversion from measured spectral radiance (in $\mu\text{W}/\text{cm}^2 \text{sr nm}$) to COD. This database is generated with the MODTRAN 5.2 atmospheric computer model maintained by the Air Force Research Lab.³ For each test site, a specific database is generated for the site altitude, surrounding surface albedo, and seasonal atmospheric model.

2.0 Data Collection

2.1 Experimental Setup

The TWST sensor was located next to the Total Sky Imager (TSI) and the Cloud Mode AERONET sensor, not far from the SAS sensors (Figure 7). The control computer was located inside the seatainer on which the SAS sensors were mounted, and a 60 ft USB cable connected it to the TWST optical head.



Figure 7. Location of TWST, AERONET, TSI and SAS at ARM Highlands site Cape Cod, MA. All sensors were heavily anchored in place to survive the high wind conditions.

³ Berk A, GP Anderson, and PK Acharya. 2011. *MODTRAN 5.2.1 Users Manual*. May.

2.2 Data Matrix

In total, data were collected on 37 different days, the first seven in a row and then the last 30 days in a row (Figure 8 and Figure 9). Because TWST uses scattered solar radiation, only daytime data are meaningful. Of these 37 days, 12 showed no appreciable clouds, 4 showed heavy clouds and rain, and the remaining 21 showed mixed clouds.

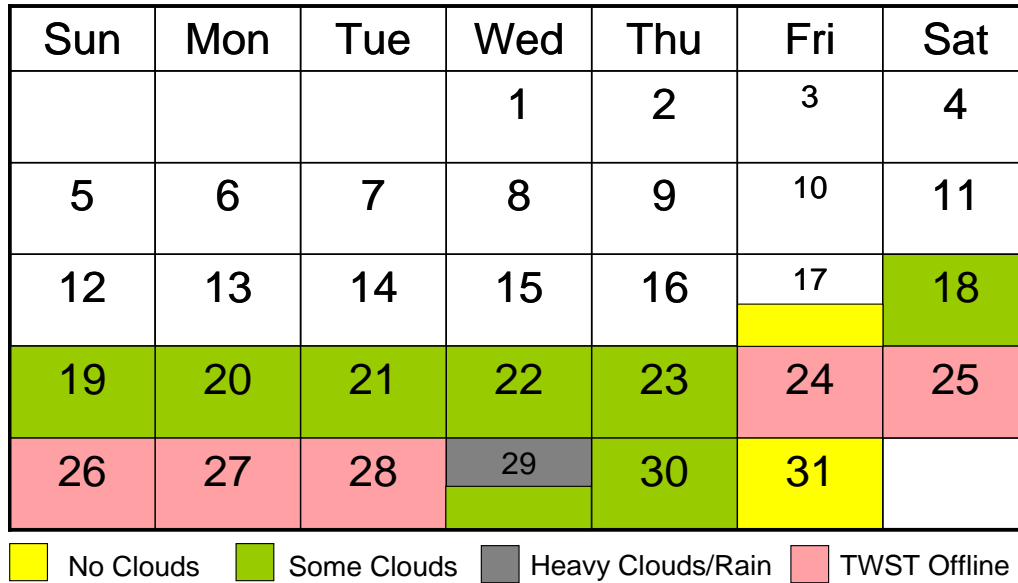


Figure 8. TWST Data Matrix for May 2013 at ARM Highlands site, Cape Cod, MA

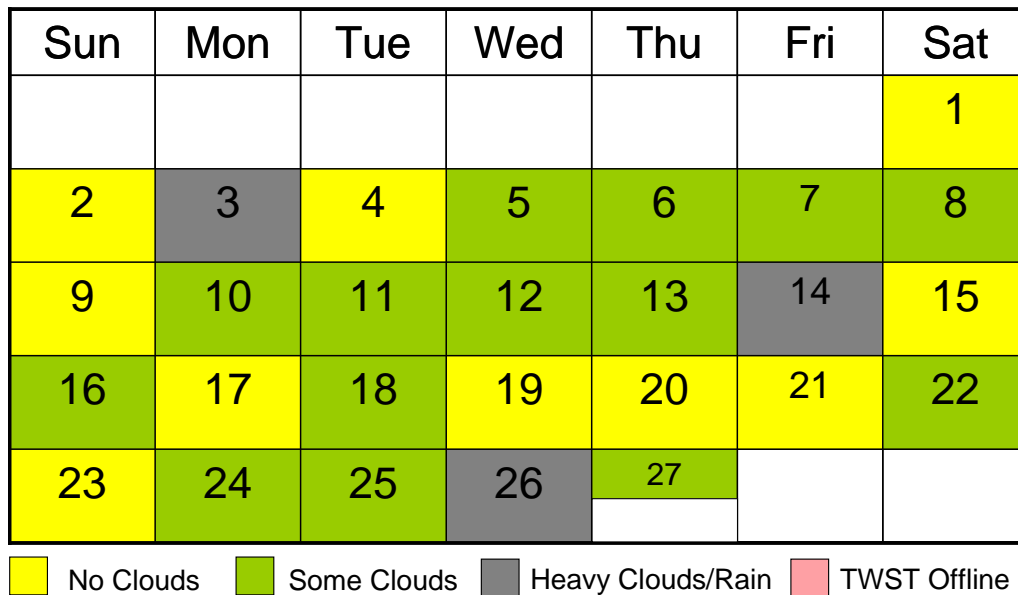


Figure 9. TWST Data Matrix for June 2013 at ARM Highlands site, Cape Cod, MA

3.0 Results

3.1 Calibration Stability

From our pre-test site survey on May 8 to our final removal of TWST from the TCAP-ARM site at Cape Cod on June 27, we executed five calibration runs at Aerodyne: May 6, May 11, May 14, May 17, and July 9 (Figure 10). For the TWST sensor, this period included two round trips to the ARM site, soak testing, and seal repairs in the lab and field that required opening the container several times with corresponding flexing of the optical fiber and re-working the shutter assembly. Through this activity, the radiometric calibration showed variation on the same level as the typical aging of the calibrated lamp in the LabSphere URS-600 calibration source. This calibration stability test has been confirmed by detailed comparisons with the AERONET spectral radiances over a period of several months.

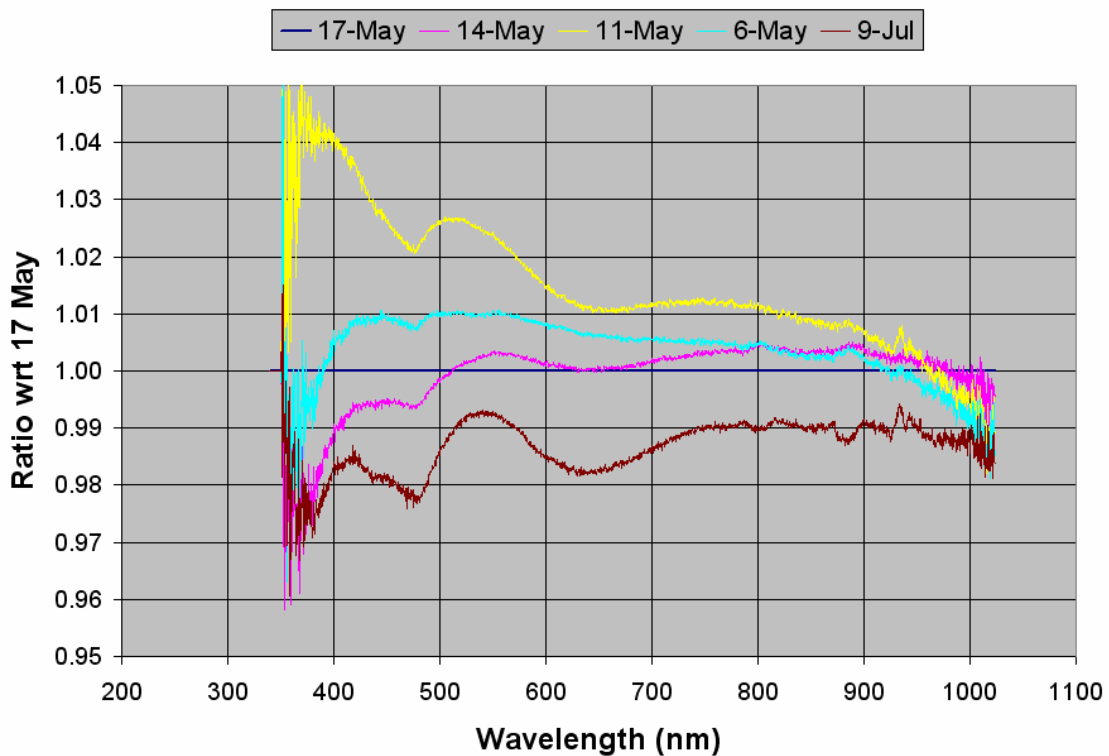


Figure 10. TWST Calibration Stability relative to calibration run on 17 May 2013.

3.2 Daily TWST Cloud Optical Depth Results

The TWST raw data (spectral radiances) were processed with a Level 1 automatic algorithm to produce COD as a function of time. The data were then plotted out for each day and examined manually for errors. A collection of digital files with the results were then prepared, one for each day (Appendix A).

3.3 Comparison to Other Sensors

As of October 2013, the available data from other AMF sensors for cost-efficient comparison with TWST are AERONET Cloud Mode, two-channel microwave radiometer (MWR), and TSI camera.⁴ We focused on the AERONET and MWR data, and used the TSI data to investigate cases where the other sensors disagreed.

3.3.1 MWR, AERONET, and TWST

Only two and a fraction days of coincident data were available for MWR comparisons (Figure 11 through Figure 15). In the morning of 18 May, the sky was clear until around 0930 EDT, at which time some very thin clouds appeared. Based on the blueness of the sky (ratio of spectral radiance at 440 nm and 870 nm), TWST assigned default minimum COD values of 0.01 for blueness above 5 and 0.02 for blueness between 2 and 5, where the spectral radiance is below the lowest value for which its MODTRAN table contains data. No AERONET Cloud Mode data are available for this time, which is consistent with the low COD values. MWR COD values were inferred from its retrieved liquid water path (LWP) values in the usual way by assuming a 4 μm droplet effective radius.⁵ The generally accepted uncertainty in MWR retrieved LWP of 0.025 mm equates to an inferred COD uncertainty of approximately 9%.⁶ An 8 μm radius would reduce the 4 μm -inferred COD and its uncertainty by half. By looking at the TSI imagery during these periods, it is apparent that no significant clouds are present, consistent with TWST and MWR (given its uncertainty bound). Similar the behavior when no clouds are present having optical depths high enough to account for the MWR, COD values have been observed in other studies.⁷

In the afternoon, the thin clouds continued (Figure 12). At approximately 1530 EDT, some heavier clouds appeared (detected by TWST and MWR) and lingered for about 2 hours. One AERONET point also exists for 1540 EDT with a value of OD 11.8, which is in reasonable agreement with the TWST value (OD 8.17) and the MWR value (OD 13.5) at that time. Afterward, the sky returned to thin clouds.

⁴ For descriptions of these sensors, refer to the following: ARM Climate Research Facility. October 1, 2013. "ARM Instruments." <http://www.arm.gov/instruments>. [[Or the most appropriate date that this was accessed]]

⁵ Stephens, GL. 1978. "Radiation Profiles in Extended Water Clouds. II: Parameterization Schemes." *Journal of Atmospheric Sciences* 35: 2123–2132, [http://dx.doi.org/10.1175/1520-0469\(1978\)035%3C2133:RPIEWC%3E2.0.CO;2](http://dx.doi.org/10.1175/1520-0469(1978)035%3C2133:RPIEWC%3E2.0.CO;2).

⁶ Cadetdu, MP, JC Liljegren, and DD Turner. 2013. "The Atmospheric Radiation Measurement (ARM) program network of microwave radiometers: instrumentation, data, and retrievals." *Atmospheric Measurement Techniques* 6: 2359–2372, [doi:10.5194/amt-6-2359-2013](https://doi.org/10.5194/amt-6-2359-2013).

⁷ Chiu, JC, A Marshak, Y Knyazikhin, WJ Wiscombe, HW Baker, JC Barnard, and Y Luo. 2006. "Remote sensing of cloud properties using ground-based measurements of zenith radiance." *Journal of Geophysical Research* 111(D16201), [doi:10.1029/2005JD006843](https://doi.org/10.1029/2005JD006843).

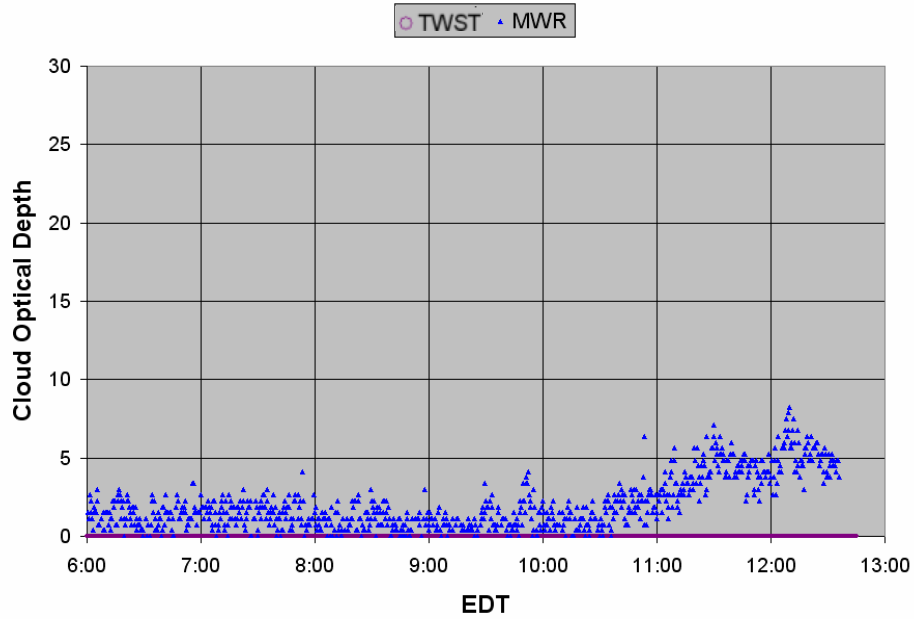


Figure 11. Comparison of CODs between TWST and MWR on 18 May 2013 in the morning. The MWR inferred COD uncertainty here is ~ 9 , consistent with clear-sky reading by TWST confirmed by TSI data.

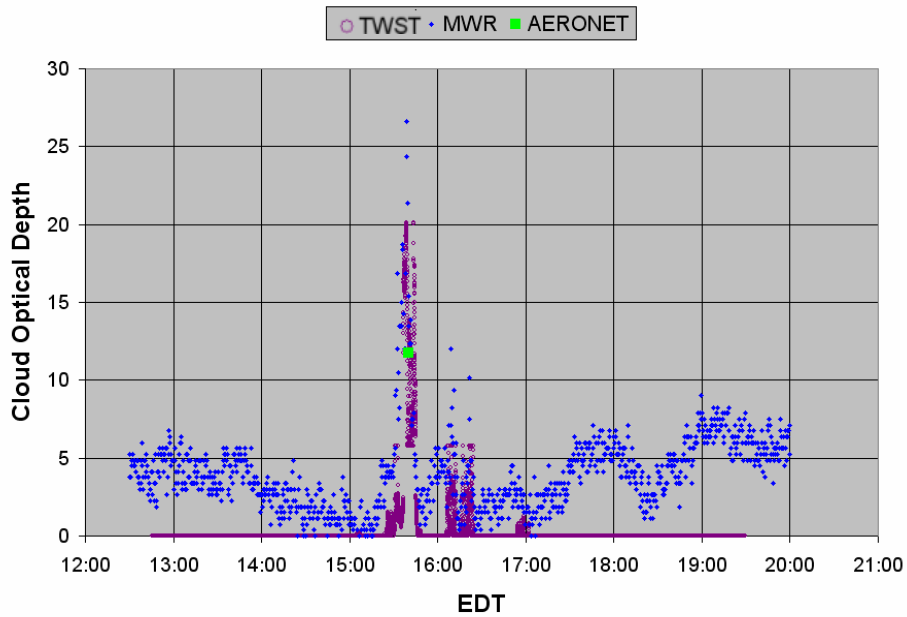


Figure 12. Comparison of CODs between TWST, MWR, and AERONET on 18 May 2013 in the afternoon. The MWR inferred that CODs within uncertainty bounds (~ 9) are consistent with TWST.

On 19 May, the cloud pattern was similar to the previous day. The morning was clear (Figure 13), but some thicker clouds appeared in the afternoon (Figure 14). The Level 1 TWST algorithm seemed to have trouble with the afternoon clouds on this day. During the times when AERONET reported COD values, the TWST values were generally close, but there is a period between 1500 and 1700 EDT where the TWST results are seemingly erroneously high, and the MWR values agreed better with AERONET than TWST. Specifically, the rapid changes, up at 1500 and down at 1700 EDT, suggest an error in the thick/thin state determination by the TWST Level 1 algorithm. We are still investigating this case and intend to make the necessary changes in the automated state determination algorithm.

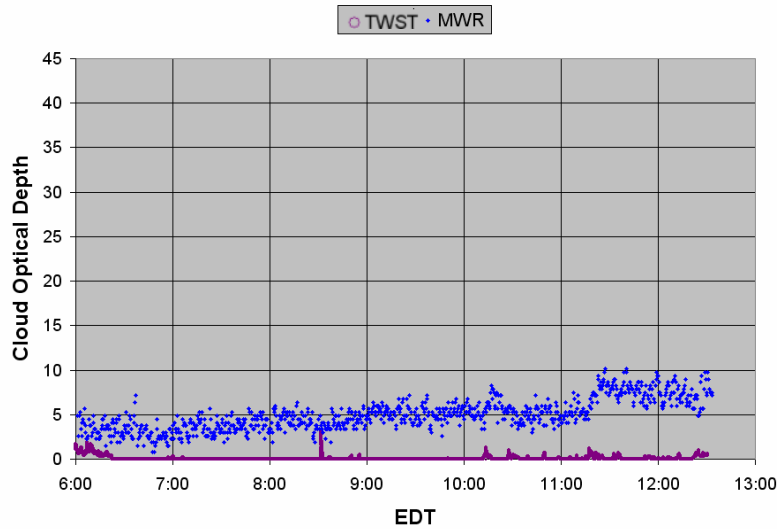


Figure 13. Comparison of CODs between TWST and MWR on 19 May 2013 in the morning. The MWR inferred CODs within uncertainty bounds (~ 9) are consistent with TWST.

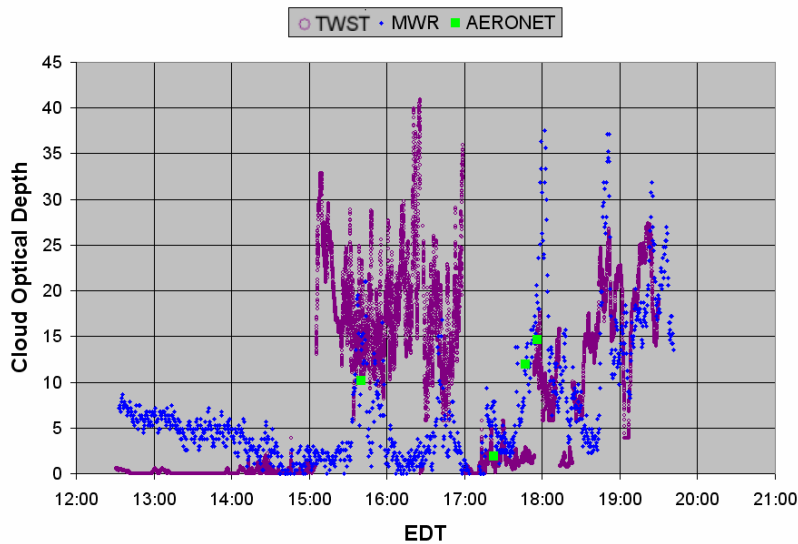


Figure 14. Comparison of CODs between TWST, MWR, and AERONET on 19 May 2013 in the afternoon.

On 20 May, the MWR was taken offline around 0830 EDT (Figure 15). The clouds from the previous day persisted overnight and gradually cleared around 1100 EDT. For the brief period of overlap with TWST and AERONET, which closely agreed with each other, the MWR inferred COD values were considerably higher. MWR recovery from its wet-window dryer, which was in operation earlier, does not seem to explain the elevated COD values. Similar disagreements between MWR and AERONET have been found in other studies.⁹ In particular, the MWR retrieval uncertainty for thin cloud and no cloud cases can be quite high.

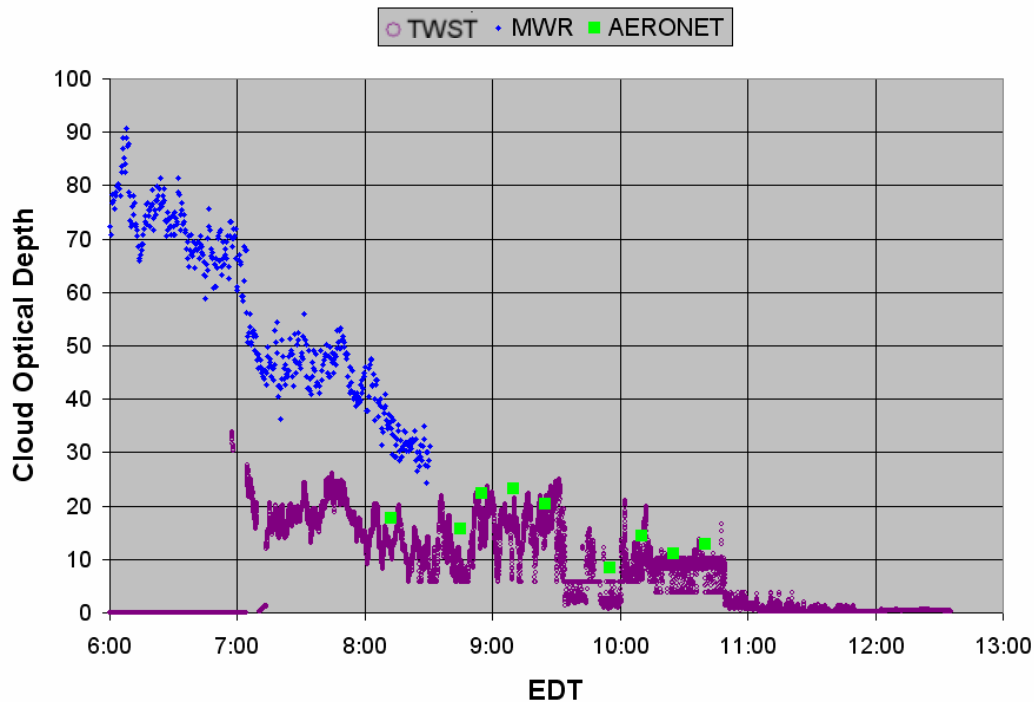


Figure 15. Comparison of CODs between TWST, MWR, and AERONET on 20 May 2013 in the early morning.

3.3.2 AERONET and TWST

For each of the times when both TWST and AERONET Cloud Mode data were available, the values were compared. In this analysis, the TWST and AERONET measurements were corrected for relative clock skew. The cases in which they disagreed were investigated using available supporting data. A summary of these comparisons is presented below, including our estimate of which of the two values is probably correct when such a determination is possible. To explain how these determinations were derived, consider a case where AERONET was probably correct, 12 June at 1738 EDT. AERONET and TWST agree (Figure 16) fairly well for the heavy clouds around 1500 EDT, but at 1738, AERONET shows a low COD while TWST yields a value of OD 60. Examination of TSI images during the AERONET measurement (Figure 17) show that a blue sky hole appeared briefly at this time, consistent with the AERONET COD value. The blueness value of 13.3 also indicates blue sky at this time. We ran some tests with a faster response time on the blue sky filter and determined that the value used for the Level 1 run was too slow for the rate at which the COD changed in this case, leading to the erroneous value for TWST.

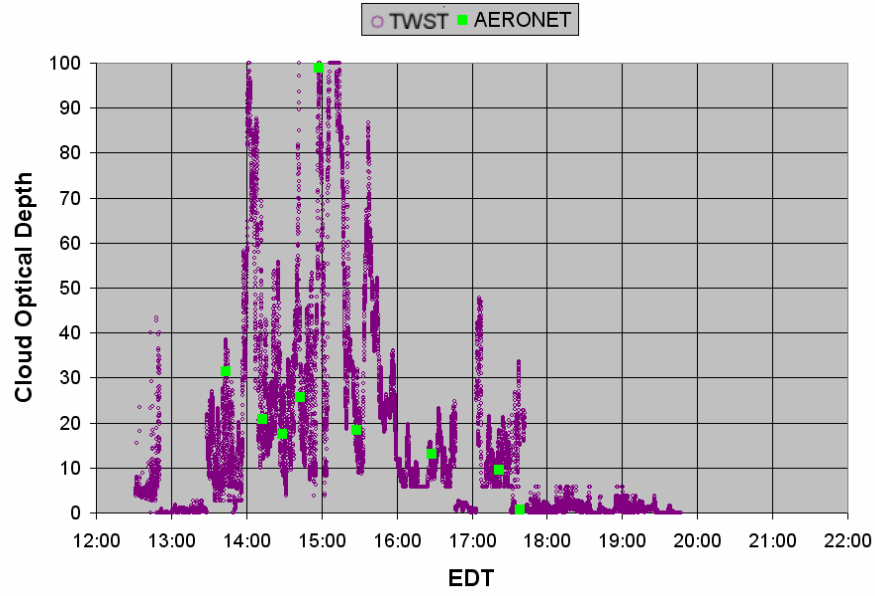


Figure 16. Comparison of CODs and related parameters between TWST and AERONET on 12 June 2013 in the afternoon.

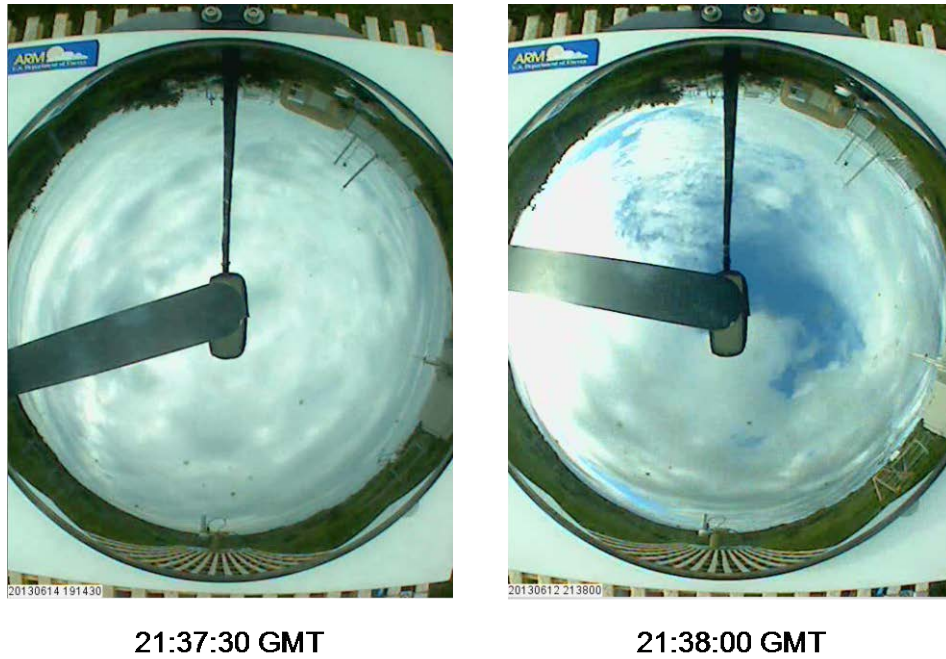


Figure 17. TSI images of the sky at ARM Highlands on 12 June 2013 at two times during the collection of AERONET data at 21:38 GMT.

A case occurred on 14 June, in which TWST probably did a better job than AERONET. In the afternoon (Figure 18) at 15:13:23, AERONET reports a value of OD 0.8, which is optically thin. TWST gives OD 27.5, which is optically thick. If TWST had decided that the clouds were optically thin, it would have reported OD 0.2, not that far from the AERONET value. The disagreement between TWST and AERONET is purely a function of the cloud state (i.e., thick [TWST] or thin [AERONET]). As in the previous case, the TSI images around this time (Figure 19) do not prove the clouds are optically thick, but the lack of any blue or bluish patches is indicative of thick clouds. The nose plot for this period (Figure 20) is more conclusive and shows the characteristic behavior of thick clouds, indicating that the TWST value is probably correct.

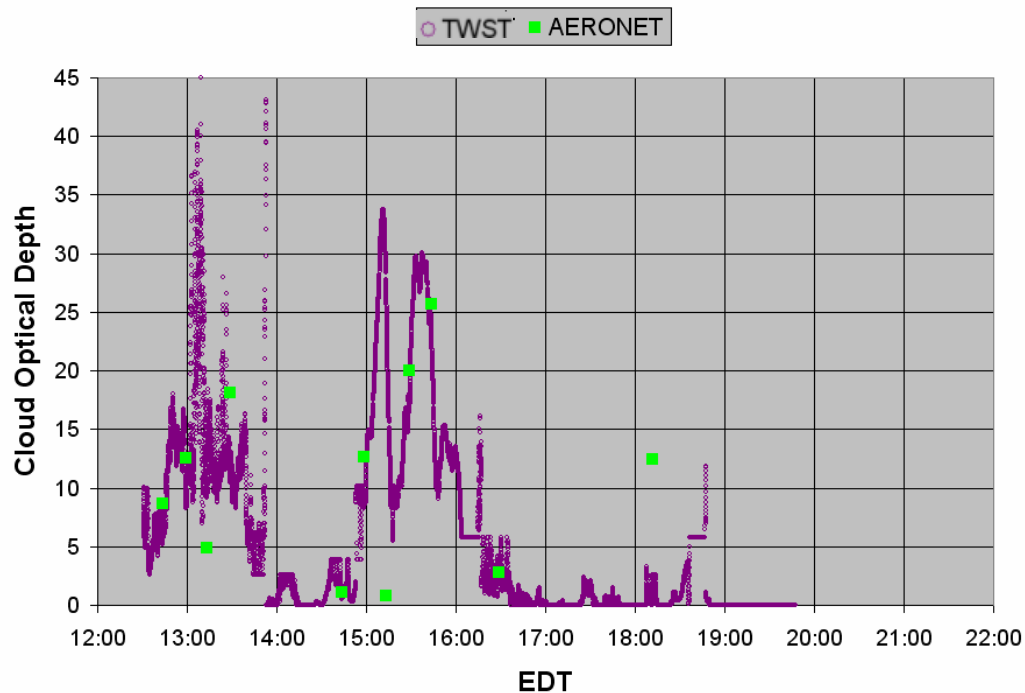


Figure 18. Comparison of CODs between TWST and AERONET on 14 June 2013 in the afternoon.

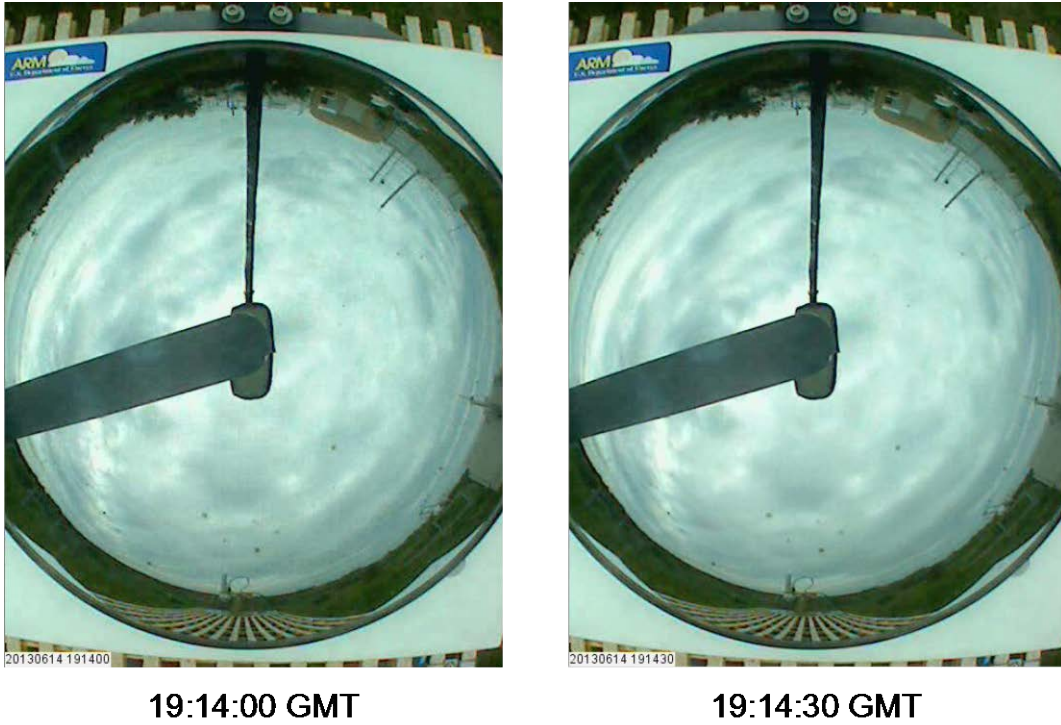


Figure 19. TSI images of the sky at ARM Highlands on 14 June 2013 at the times of collection of AERONET data at 19:14 GMT.

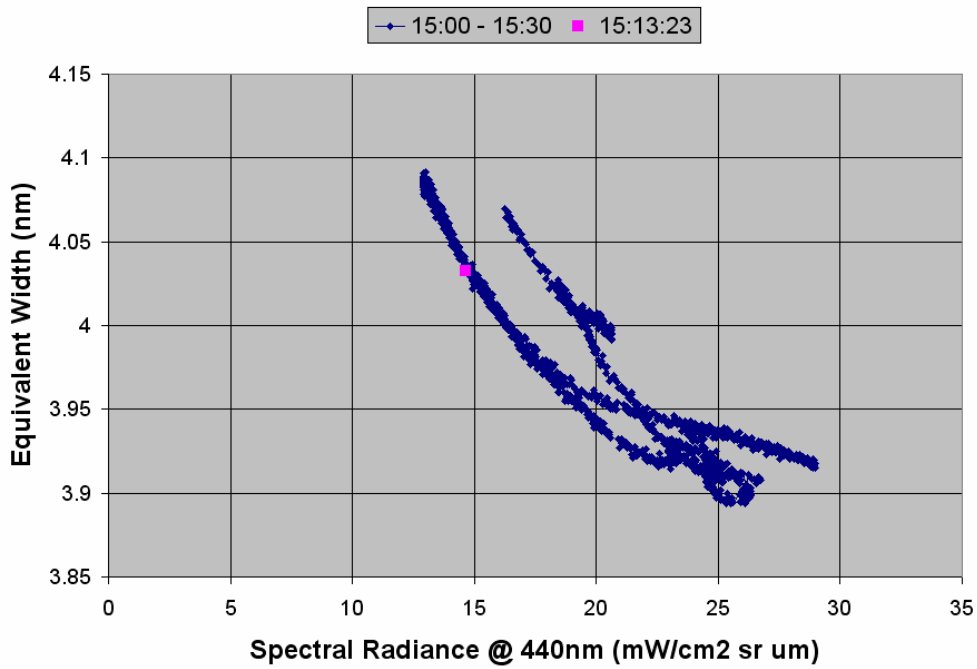


Figure 20. Nose Plot of TWST measurements for the 30 minutes containing the time of the AERONET data collection on 14 June 2013 at 19:14 GMT (15:13:23 EDT). The pink square shows the TWST point that matches the 15:13:23 EDT AERONET measurement.

Another effect, AERONET time averaging, also causes disagreements between the AERONET Cloud Mode COD values and those of TWST. A comparison of the spectral radiances measured by AERONET and TWST (Figure 21) shows close agreement. A significant radiance jump occurred near the middle of this AERONET measurement around 12:58:30 EDT, which just happened to overlap with a TWST dark current measurement. The corresponding cloud optical depths (Figure 22) show that the AERONET Cloud Mode value at the stated time of the AERONET measurement, OD 24.7 agrees with the TWST value after the jump but not with the TWST value at the stated time, OD 47.8.

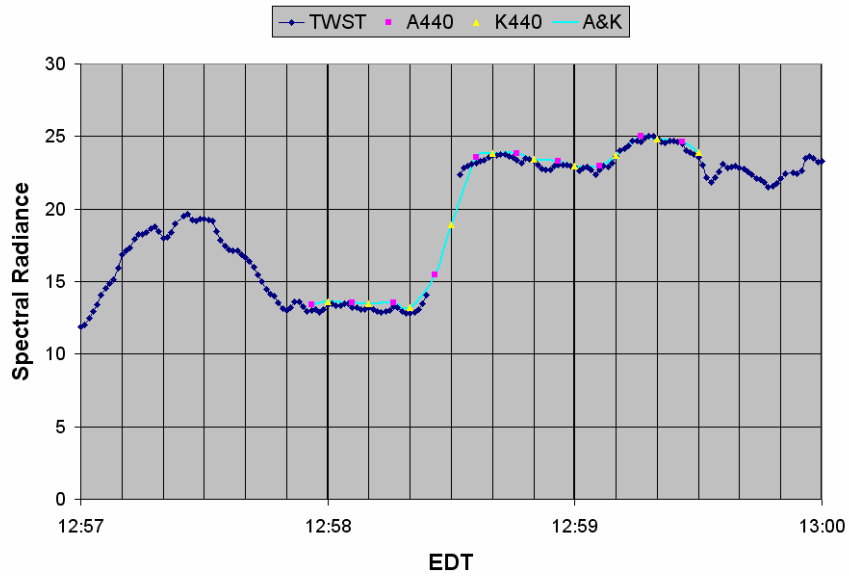


Figure 21. Spectral Radiance at 440 nm for AERONET Cloud Mode (A440 and K440) and TWST.

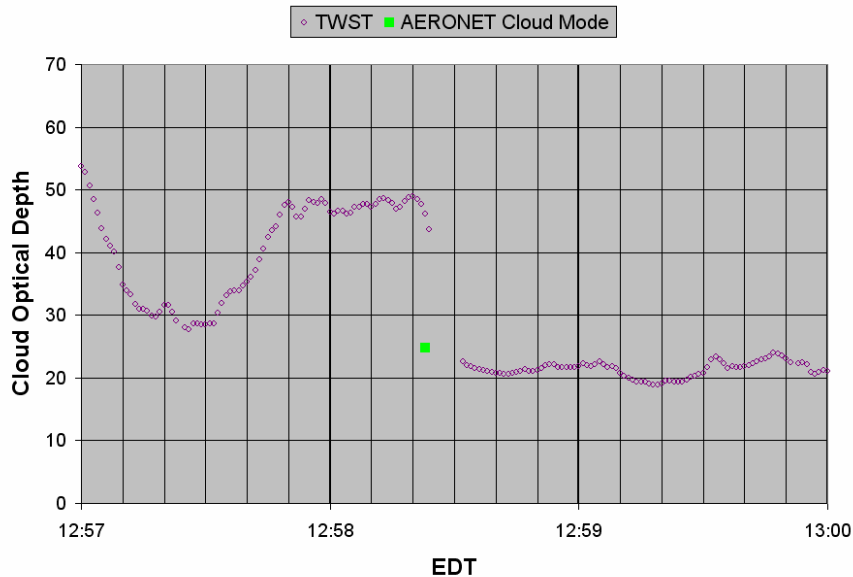


Figure 22. TWST and AERONET Cloud Mode CODs corresponding to the spectral radiances in Figure 21.

We must point out, however, that the few points of disagreement between AERONET and TWST on which we have focused in this section are interspersed with many more points of agreement, both optically thin and optically thick cases. The summary plot of all the AERONET measurements during the test period (Figure 23) makes this point quite convincingly. The majority of the primary points of disagreement, some in which TWST is probably correct and others where AERONET is probably correct, occur where the sensors have chosen different optically thick/thin states. This is a direct result of the COD ambiguity. Several occur at times when the clouds are known to deviate from the 1D assumption, making both AERONET and TWST values somewhat unreliable. In addition, the nature of the AERONET Cloud Mode algorithm tends to under-sample optically thin states, eliminating many times when the two sensors would have shown close agreement.

One finding herein suggests an easily implemented improvement to the AERONET Cloud Mode algorithm. Cases for which AERONET erroneously reports a low-value optical depth might be fixed by employing a “blueness measure,” or the ratio of 440 nm/870 nm radiances (section 2.1.1 and section 4.3.2). Overhead measurements with low blueness are most likely not low optical depth.

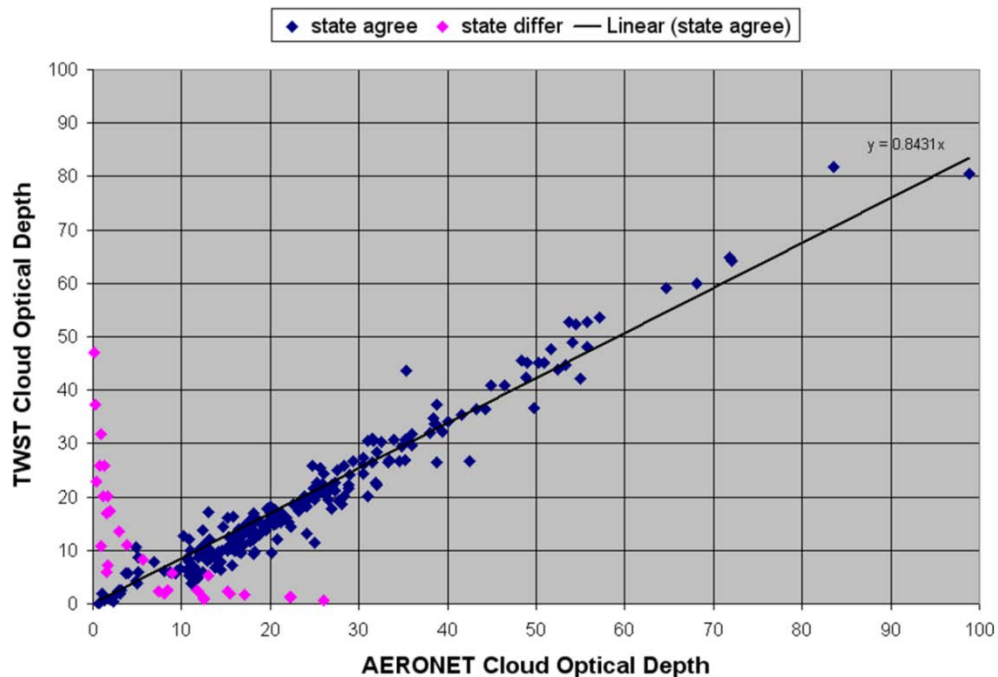


Figure 23. Comparison of AERONET Cloud Mode to TWST Cloud Optical Depths for a 37-day field measurement period. Cloud state refers to the “thick or thin” choice made by the AERONET and TWST COD retrieval algorithms. To make this comparison correctly, one must understand the “trimmed mean” technique used by the AERONET Cloud Mode to extract a single value from the 10 points collected in each 90-sec sample period.

As explained in section 1.0, we generated this comparison in Figure 23 between AERONET CM and TWST COD measurements by performing the same “trimmed mean averaging” of the TWST data that are used by the AERONET CM.⁹ The results plotted in Figure 23 show the excellent agreement between the independent COD measurements obtained by TWST and the AERONET CM sensors with an rms-deviation of OD 3.2.

4.0 Conclusions

After water-proofing the container and making a few minor electrical adjustments associated with the dark baseline shutter mechanism, TWST was stable over the final month of the test. This determination included an excellent radiometric stability, plus or minus a couple percentage points. Although accuracy during active rainfall could not be confirmed with the auxiliary data available, the TWST data appear reasonable (high cloud optical depths during heavy rain) and show no ill effects for measurements soon after the rain stopped. The slanted window design, frequent checking, and rinsing with distilled water prevented any significant degradation over time.

Comparison of TWST cloud optical depths to those from MWR and AERONET verified the field-worthiness of TWST. The use of the equivalent width of the oxygen A-band near 760 nm enabled the application of the nose plot to resolve the COD ambiguity, a persistent issue characteristic of all radiance-based sensors.

The scant 2 days of overlap between TWST and MWR present issues requiring further investigation. The afternoon of 19 May (Figure 14) produced many TWST readings that are probably too high, e.g., the periods between 1500 and 1600 EDT, based on the close agreement between MWR and AERONET where they overlap. We believe the cause of this particular discrepancy resides in the automated thick/thin cloud state determination by TWST. We are confident this type of error will be dealt with successfully once we have fully incorporated the equivalent width information into our automated decision algorithm.

Overall the agreement between AERONET and TWST was excellent, as in our previous comparisons. This field test opportunity has provided us direction for improving our Level 1 data processing algorithm to make it adhere more closely to investigator analysis based directly on the oxygen A-band Equivalent Widths (or our so-called nose plots) instead of relying solely on the slope information captured by the Level 1 filter algorithms.

Appendix A: TWST Digital Data Description

For each day of significant data collection, a digital file was prepared of the TWST data. Each file has the name: fitsOut_{date}.csv, where {date} is in the format of {day of month}{month}, e.g. fitsOut_17May.csv or fitsOut_27June.csv. As the file extension indicates, the files are comma separated values with six columns. The first line of each file contains column headings, DATE,SR440,SR870,EQW,Sza,RatCOD. The quantities in each column are:

DATE	the date and time of the data point (e.g. Sat Jun 01 04:49:21 EDT 2013),
SR440	the spectral radiance at 440 nm in units of ($\mu\text{W}/\text{cm}^2 \text{ sr nm}$) or ($\text{mW}/\text{cm}^2 \text{ sr } \mu\text{m}$),
SR870	the spectral radiance at 870 nm in units of ($\mu\text{W}/\text{cm}^2 \text{ sr nm}$) or ($\text{mW}/\text{cm}^2 \text{ sr } \mu\text{m}$),
EQW	the equivalent width of the oxygen A-band from 750 - 785 nm in units of (nm),
Sza	the Solar Zenith Angle in degrees (0 is straight up),
RatCOD	the TWST Cloud Optical Depth.

The COD is defined as the integral of the extinction coefficient at 550 nm, as a function of altitude, from the ground to the top of the atmosphere for a vertical path.

In the digital files a value of RatCOD = -1 is used to indicate that the TWST Level 1 data processing algorithm was unable to assign a value for that particular time. In most cases this is due to the fact that the Level 1 algorithm only works for solar zenith angles between the limits used to generate the lookup table. In addition, certain times where the solar zenith angle is within the table's range but the measured spectral radiances and equivalent width do not allow the algorithm to assign a value.

Similarly a default value of OD 0.01 is assigned for every case of blue sky, and a value of 0.02 is assigned for every non-blue sky case of spectral radiance at 440 nm that is below that of the least bright optically thin point in the lookup table. A value of 100 is assigned for each case of spectral radiance at 440 nm that is below that of the least bright optically thick point in the lookup table (refer to Figure 3 for explanation of these quantities).

Appendix B: TWST Cloud OD Sensor Specifications

TWST Cloud OD Sensor Specifications	
Weight	20 lbs
Power	4 hour battery life, or continuous with AC power source for control computer
Size	11" x 8" x 8" plus 12" external sun baffle; or 11" x 12" x 8" with internal sun baffle
Operating Range	Blue Sky to Cloud OD 100
Cloud OD Precision	1% (typical, depends on update rate)
Cloud OD Sensitivity	0.005 for Optically Thin Clouds
Power for Sensor 5 Vdc	One USB cable connection to computer (power and data)
Environmental Container	NEMA 4 sealed enclosure
Precipitation	Slanted optical window design drains water
Data Logging Rate	1 Hz (typical), variable sampling interval from 0.1 to 120 sec
FOV	0.5 deg
Spectral Range, Resolution	350 – 1000 nm, ~2 nm
Spectral Bands used in Cloud OD retrieval	440, 761, and 870 nm



U.S. DEPARTMENT OF
ENERGY

Office of Science